

Direct measurement of force between colloidal particles in a nematic liquid crystal

This article has been downloaded from IOPscience. Please scroll down to see the full text article.

2008 J. Phys.: Condens. Matter 20 075106

(<http://iopscience.iop.org/0953-8984/20/7/075106>)

View [the table of contents for this issue](#), or go to the [journal homepage](#) for more

Download details:

IP Address: 129.252.86.83

The article was downloaded on 29/05/2010 at 10:33

Please note that [terms and conditions apply](#).

Direct measurement of force between colloidal particles in a nematic liquid crystal

Kenji Takahashi, Masatoshi Ichikawa and Yasuyuki Kimura¹

Department of Physics, School of Sciences, Kyushu University, 6-10-1 Hakozaki, Higashi-ku, Fukuoka, 812-8581, Japan

E-mail: ken8scp@mbox.nc.kyushu-u.ac.jp and kim8scp@mbox.nc.kyushu-u.ac.jp

Received 10 August 2007, in final form 20 November 2007

Published 25 January 2008

Online at stacks.iop.org/JPhysCM/20/075106

Abstract

The interparticle force between two colloidal particles in a nematic liquid crystal is directly measured as a function of the interparticle distance R by two different experimental methods: the free-release method and the optical tweezing method. The obtained force between an elastic ‘dipole’, which constitutes a colloidal particle and an accompanying hyperbolic hedgehog defect, confirms previous theoretical predictions that the force is attractive and proportional to R^{-4} . We also observe that a repulsive component emerges at short distances to preclude direct contact of the particles. We find that the magnitudes of the forces obtained by the two methods are different. The origin of this discrepancy is discussed by a comparison between the static and the non-static measurements.

1. Introduction

The interaction between colloidal particles in a structured fluid such as a liquid crystal or polymer solution has recently attracted the attention of many researchers from both fundamental and applied points of view. A colloidal particle located in a nematic liquid crystal breaks the continuous rotational symmetry of the medium. When the surface anchoring of the particle is sufficiently strong, the particle becomes an orientational (topological) defect. At the same time, another defect emerges near the particle to restore the orientational order far from the particle [1–4]. Furthermore, a long-range specific interaction mediated by the orientational elasticity of the liquid crystal appears between these particles, even if the particles exhibit no direct interaction with each other. This specific interaction depends on the type of defect pair and the orientation of the liquid crystal at the particles’ surfaces [2–5]. In this paper, we directly measure the specific long-range interaction between two particles with strong normal anchoring in a nematic liquid crystal.

In our case, the particle becomes a topological defect called a radial hedgehog defect, and another defect called

a hyperbolic hedgehog defect emerges near the particle to conserve the far-field director of the liquid crystal, as shown in figure 1 [2–4]. Lubensky *et al* showed that this type of particle–defect pair can be regarded as a dipole because of its shape and analogous behaviour [2]. Defining the interparticle distance as the center-to-center distance R , the dependence of the interparticle force F on R is similar to that between electric dipole moments.

In particular, when two pairs of elastic dipoles are aligned parallel to the far-field director, as shown in figure 1(b) (parallel configuration), F is predicted to be attractive and proportional to R^{-4} [2, 4]. This theoretical prediction has been examined by various experiments [6–8]. Droplets of ferrofluid in a nematic solvent under a tunable magnetic field were used in one of the previous experiments [6]. In the other experiments, optical [7] and magnetic tweezers [8] were used. All experiments show that F is proportional to R^{-4} . However, there is a quantitative difference between the experimental results for the magnitude of the interparticle force. In this study, we measured the force F in the parallel configuration, as shown in figure 1(b), and the force measurement was performed using two experimental methods (free release and optical tweezing) for the same particle pairs.

¹ Author to whom any correspondence should be addressed.

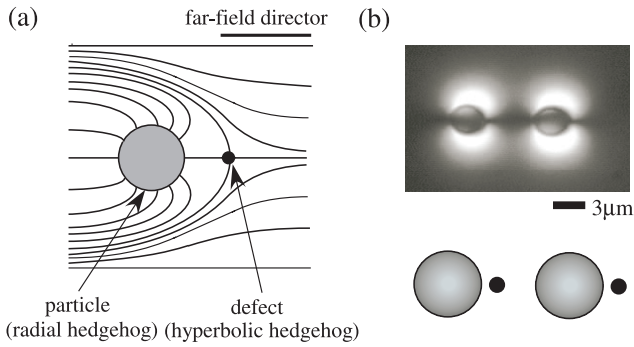


Figure 1. Elastic dipole moment composed of a particle and its accompanying defect in a nematic liquid crystal. (a) Schematic illustration of an elastic dipole moment. Its direction is parallel to the far-field director. The solid lines represent the director field. (b) Cross-Nicol polarizing microscope image of two elastic dipole moments in parallel configuration.

2. Experiment

We used polystyrene latex particles (radius $a = 1.5 \mu\text{m}$, Magsphere Inc.) and MJ032358 (Merck Japan) as a nematic liquid crystal. The particles were coated with octadecyldimethyl (3-trimethoxysilylpropyl) ammonium chloride (DMAOP) to promote homeotropic anchoring at their surfaces. The particles and the liquid crystal were simply mixed and sandwiched between glass plates. The surfaces of the glass plates were coated with polyimide and rubbed in one direction to attain homogeneous alignment of the liquid crystal. The thickness of the sample cell was fixed at $10 \mu\text{m}$ using spacer films.

Optical tweezing is a useful tool for manipulating micrometer-sized particles in a solution whose refractive index is smaller than that of the particles [9]. We used dual beam optical tweezers [10] to manipulate two particles within a two-dimensional plane and to measure the force directly. Since the refractive index of the latex particles is 1.6 and the ordinary and extraordinary refractive indices, n_o and n_e , of the liquid crystal are respectively $n_o = 1.46$ and $n_e = 1.5$, a particle can be stably trapped in any direction. The trapping beam of a Nd-YVO₄ laser (Spectra Physics, wavelength 1064 nm) was introduced into an inverted microscope (TE2000U, Nikon) and focused by a 100× oil immersion objective lens (N.A. = 1.3). The position of one laser spot was controlled by two Galvano mirrors (model 6450, Cambridge Technology Inc.), and the other spot was fixed. The Galvano mirrors were controlled using a function generator (NF1946). We used a video microscope to capture the motion of the particles.

For the free-release measurement, we used a similar method to that described in reference [6]. We selected two distant particles in the parallel configuration and aligned them parallel to the far-field director using the optical tweezers. After turning off both laser beams, we captured the motion of the two particles until they came to rest. The force was calculated from the approaching velocity of the particles and the viscosity of the liquid crystal parallel to the director [6]. Although in the previous study, the macroscopic average viscosity was used at the evaluation process, in this study we directly measured the effective viscosity of the liquid crystal

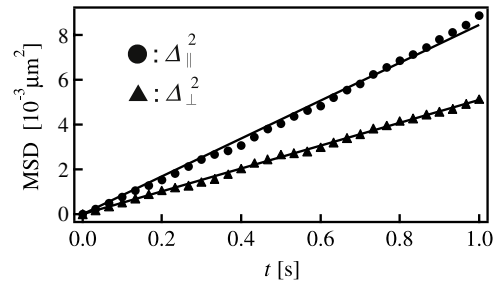


Figure 2. Temporal evolutions of the mean square displacement (MSD). The MSDs of a particle parallel Δ_{\parallel}^2 and perpendicular Δ_{\perp}^2 to the far-field director are represented by filled circles and filled triangles, respectively. We can evaluate the viscosities η_{\parallel} and η_{\perp} from the slopes of the best-fit lines.

parallel to the director from the Brownian motion of the same particle [11].

We also used dual beam optical tweezers to measure the static interparticle force directly. Although the force has already been measured by optical tweezers [7], we measured it continuously using a different method. If a particle receives no external force, it stays at the bottom of the optical potential. When the particle receives an external force, it shifts to the position where the external force balances the optical trapping force. Therefore we can obtain the interparticle force F from the displacement of the fixed particle. In this experiment, we moved the laser spot slowly to vary R and measured the displacement of the particle by analysis of the microscope images.

3. Results

3.1. Free-release measurement

From the Brownian motion of a single particle, we can measure the local viscosity of the liquid crystal by the following method. We captured an image of the particle using a CCD camera (ADT-33B, Flovel), and calculated its center position. Since the particle is accompanied by a large deformed area around it, as shown in figure 1(b) (white region), we used bright-field images of the particle for analysis. The temporal evolutions of the mean square displacement (MSD) of a particle along and perpendicular to the director, Δ_{\parallel}^2 and Δ_{\perp}^2 , are shown in figure 2. The self-diffusion constant of the particle along the far-field director D_{\parallel} is given by the Stokes–Einstein relation $D_{\parallel} = k_B T / 6\pi\eta_{\parallel}a$ [12], where η_{\parallel} is the viscosity along the far-field director, k_B is the Boltzmann constant and T is the temperature. Since Δ_{\parallel}^2 is proportional to the elapsed time t and is theoretically given as $\Delta_{\parallel}^2 = 2D_{\parallel}t$, the slope of the best-fit line in figure 2 corresponds to $2D_{\parallel}$. We obtained the viscosities parallel and perpendicular to the far-field director as $\eta_{\parallel} = 1.73 \times 10^{-2} \text{ Pa s}$ and $\eta_{\perp} = 3.04 \times 10^{-2} \text{ Pa s}$, respectively. Under the assumption of a steady condition, the frictional force exerted on a particle balances the interparticle force F . Therefore, we can obtain F from the viscosity and the approaching speed of the two particles, v .

Disregarding the Brownian motion, the particles approached each other along the far-field director. The obtained

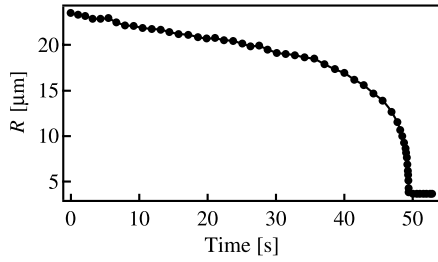


Figure 3. Time evolution of the interparticle distance R . R decreases as the time elapses. Once R reaches about $3.7 \mu\text{m}$, the particles stop.

temporal change of the interparticle distance R is shown in figure 3. It is indicated that the attractive interaction is dominant at a distance of at least eight times the diameter of a particle. The interparticle force in the nematic liquid crystal is quite long-range and much stronger than ordinary forces such as the van der Waals and screened Coulomb forces acting in an aqueous solution. The distance R monotonically decreases as time elapses until R reaches about $3.7 \mu\text{m}$. After that, R does not change further. Although R would be $3 \mu\text{m}$ if the particles were in direct contact, there is a point defect between them, as mentioned before. This defect prevents the particles from coming into direct contact. The equilibrium distance between a particle and its defect is expected to be as large as $0.2a$ according to theoretical studies [2, 4]. Since the theory predicts the stable distance between the two particles R to be $3.6 \mu\text{m}$ in our case, this prediction is in good agreement with our experimental result. From figure 3, we can calculate the approaching speed v by numerical differentiation. During the approach, we also notice that the speed is slightly different for the two particles depending on the arrangement of the particle-defect pair, regardless of there being no net flow in the liquid crystal matrix. The right particle is faster than the left one in the arrangement shown in figure 1.

Assuming that F is equal to the frictional force, we can obtain $F = 3\pi\eta_{\parallel}av$, as shown in figure 4. The force F is plotted using a logarithmic scale in the inset of figure 4. The force is attractive at all distances between two moving particles and is proportional to R^{-4} except at short distances. Taking into consideration the higher multipole moments in the electrostatic analogy [9], F is represented by the sum of the dipolar component (R^{-4}) and the quadrupolar component (R^{-6}); $F = -\alpha R^{-4} + \beta R^{-6}$, where α and β are the parameters representing the magnitudes of the dipolar and the quadrupolar components, respectively. Since the quadrupolar component is much smaller than dipolar component in the theory, we do not expect to observe a repulsive term. However, at short distances, a clear deviation from the theoretical force curve appears in the experimental result, and a strongly repulsive component emerges. One possible origin of this repulsion is the deformation of the hyperbolic hedgehog defect between the particles when R becomes small. However, we cannot determine the origin of this repulsive component easily by this experiment, because there is some complexity and uncertainty in this method, as discussed below.

In the free-release method, we assume that the viscosity is independent of the interparticle distance R and is equal to

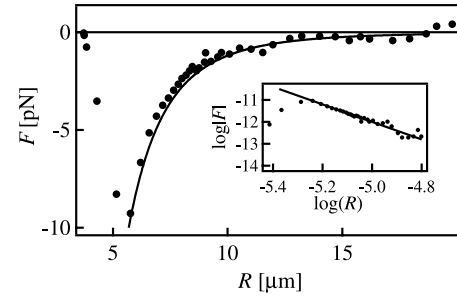


Figure 4. Dependence of interparticle force F on the interparticle distance R obtained by free-release measurement. A negative sign indicates an attractive force. The solid line is the curve $F = -\alpha R^{-4} + \beta R^{-6}$ proposed by Lubensky *et al* [2]. The inset is a logarithmic plot, and the slope of the solid line is -4 .

that obtained from the Brownian motion. For large R , this assumption is expected to hold well. However, for small R , the orientation of the liquid crystal between the particles differs from that for large R . Therefore, the effective viscosity for small R will be different from that for large R (viscosity probably depends on R and takes an intermediate value between η_{\parallel} and η_{\perp}). We also assume that the interparticle force is equal to the frictional force. The velocity of a particle increases for short R and the system is no longer stationary. In addition, the nematic host cannot escape quickly from the region between the particles. This hydrodynamic effect seriously affects the obtained interparticle force in the free-release method. Moreover, it is not easy to subtract these undesirable effects from the obtained data. Therefore, to measure the interparticle force originating from the elastic deformation alone, we should use any other method for which the results do not depend on the viscosity and is as free from the hydrodynamic effect as possible.

3.2. Dual-beam optical tweezing measurement

We also adopted a method using dual-beam optical tweezers, because the results obtained do not depend on the viscosity or the hydrodynamic effect. First, we measured the trap potential of the optical tweezers. The distribution of a trapped particle's position gives direct information on the potential profile [10]. Since the obtained distribution is well described by a Gaussian, we regard the trapping potential obtained using the tweezers as being harmonic. From the Boltzmann relation, the probability density of the particle's position $P(x)$ is given as $P(x) = A \exp(-kx^2/2k_{\text{B}}T)$, where k is the spring constant that characterizes the harmonic potential and A is the normalizing factor. We fitted this equation to the experimental result (figure 5), and we obtained $k = 2.9 \times 10^{-5} \text{ N m}^{-1}$. Although the particles only travel to a distance whose energy is several $k_{\text{B}}T$ in the process of obtaining k , the obtained potential profile describes the whole potential profile well. We obtained a similar profile quantitatively by tracking a released particle near the potential well. The trapping potential depends on various experimental conditions including laser power and position of the particle in a cell. Therefore, a similar calibration procedure was repeated in every experimental run.

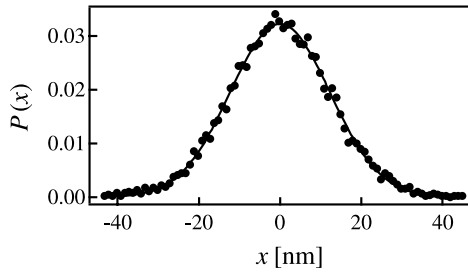


Figure 5. Probability density of the position of a trapped particle $P(x)$. The solid line is the best-fit Gaussian curve.

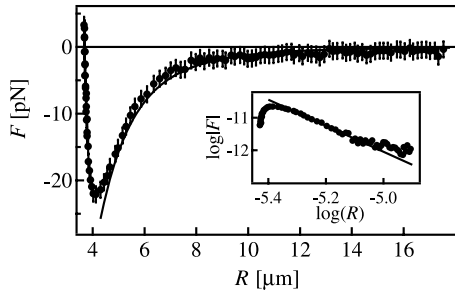


Figure 6. Dependence of the interparticle force F on the interparticle distance R . The data for both approach and withdrawal are plotted. A negative sign indicates an attractive force, and a positive sign indicates a repulsive force. The solid line is the curve $F = -\alpha R^{-4} + \beta R^{-6}$ proposed by Lubensky *et al* [2]. The inset is a logarithmic plot, and the slope of the solid line is -4 .

From the images observed under a microscope, we obtained the time evolution of the displacement of the particle trapped by the fixed tweezers while the other particle was moved at a constant speed of 60 nm s^{-1} using the optical tweezers. We calculated the interparticle force F from the displacement of the particle trapped by the fixed tweezers using the spring constant of the optical tweezers. The obtained dependence of F on R is shown in figure 6 and the bars show experimental error (approximately $\pm 1.2 \text{ pN}$) considering heat swinging. We find again that the force is attractive and nearly proportional to R^{-4} except for small R (inset of figure 6). For small R , the strongly repulsive component also emerges in this experiment. The experimental force curve deviates from that obtained from the electrostatic analogy, as shown in figure 6. This is due to the fact that two particles can approach each other when their distance is greater than their equilibrium distance. These results are qualitatively similar to those obtained by the free-release experiment. We measured the interparticle force during both approach and withdrawal, but no significant difference was found between the two results. We also decreased the speed of the laser spot (12 nm s^{-1}), but there was little difference between the two results. On the other hand, when the scanning speed increases considerably, hysteresis appears in the force curve ($F-R$) due to the hydrodynamic effect.

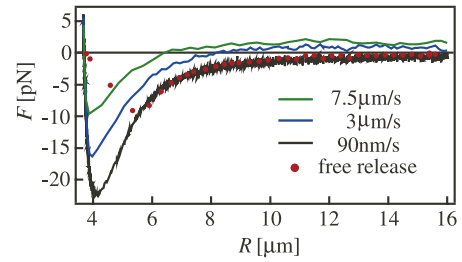


Figure 7. Dependence of the force curve on speed of a particle measured using optical tweezers. The approaching speeds are 90 nm s^{-1} (lower line), $3.0 \mu\text{m s}^{-1}$ (middle line) and $7.5 \mu\text{m s}^{-1}$ (upper line), and the filled circles represent the force curve obtained by the free-release measurement.

(This figure is in colour only in the electronic version)

4. Discussion

From the two different experimental methods, we find that F is attractive and nearly proportional to R^{-4} for large R . Regarding this point, these results are in good agreement with the reported results [6–8]. However, there is a difference between the results of the two experiments regarding the magnitude of the interparticle force. We also confirmed this difference in our experiment. In addition, we found that the force curve of the experimental results are different from ones predicted by the electrostatic analogy [9], as shown in figure 6.

The origin of this deviation is due to the hydrodynamic effect in the first experiment, as mentioned above. To evaluate this effect, we measured the force curve ($F-R$) using the optical tweezers while changing the speed of approach. The results are shown in figure 7. Each force also has the same experimental error (approximately $\pm 1.2 \text{ pN}$) as in figure 4. The effect of the variation in speed is not significant for large R . However, for small R , the magnitude of the force at the same R monotonically decreases with increasing particle speed. At a high scanning speed, the force data for large R become positive. This repulsion originates purely from the hydrodynamic interaction between the two particles due to the motion of the scanned particle generating a flow field around the particles. However, the result of the free-release experiment matches that of the optical tweezing experiment at the slowest scanning speed, even at the maximum approaching speed of $20 \mu\text{m s}^{-1}$ at $R = 6 \mu\text{m}$. Therefore, we cannot simply attribute the discrepancy between the two methods to the hydrodynamic effect alone. The cancellation of various effects may occur in the free-release method under the above conditions. From these comparisons, the measurement using the optical tweezers seems to be more reliable for evaluating the interparticle force.

A shortcoming of the optical tweezing method has recently been pointed out. Muševič *et al* [13] have reported that optical tweezers strongly deform the director field around a particle, and this makes it possible to trap a colloidal particle even if its refractive index is lower than that of the surrounding liquid crystal. In this study, we improved the optical tweezing method to diminish this shortcoming as follows. We used a laser beam that was as weak as possible. In addition, since the

size of the laser spot is smaller than the size of a particle, we could reduce this deformation effect. We also subtracted the effect of the moving laser spot on the fixed particle by carrying out a force measurement without trapping a particle. At the smallest value of R , the other spot exerts a force corresponding to an attractive force of 3 pN at the smallest value of R . Therefore, we could measure F accurately except for at the inevitable minimum deformation of the director field induced by the laser beam. The agreement of the measurement using optical tweezers with the free-release measurement at large R also suggests the validity of our optical tweezing method.

5. Conclusions

We measured the force between particles with a hyperbolic hedgehog defect in a nematic liquid crystal. The force is attractive and is nearly proportional to R^{-4} , where R is the interparticle distance. This dependence is confirmed for large R , but we observed a repulsive component when R becomes small. The origin of the quantitative difference in the magnitude of the force measured by different methods is discussed, and our improved method of optical tweezing is found to be reliable for the force measurement.

Acknowledgments

The authors thank Dr A Sawada (Merck Japan) for providing a liquid crystal sample, and Dr J Fukuda (AIST) for

valuable discussion. This work is financially supported by a Grant-in-Aid for Scientific Research from JSPS and by Grant-in-Aid for Scientific research on Priority Area 'Soft Matter Physics' from MEXT, Japan. MI was also financially supported by the Sumitomo Foundation and the Sasakawa Scientific Research Grant from the Japan Science Society.

References

- [1] Poulin P, Stark H, Lubensky T C and Weitz D A 1997 *Science* **275** 1770
- [2] Lubensky T C, Pettey D, Currier N and Stark H 1998 *Phys. Rev. E* **57** 610
- [3] Poulin P and Weitz D A 1998 *Phys. Rev. E* **57** 626
- [4] Stark H 2001 *Phys. Rep.* **351** 387
- [5] Fukuda J, Stark H, Yoneya M and Yokoyama H 2004 *Phys. Rev. E* **69** 041706
- [6] Poulin P, Cabuil V and Weitz D A 1997 *Phys. Rev. Lett.* **79** 4862
- [7] Yada M, Yamamoto J and Yokoyama H 2004 *Phys. Rev. Lett.* **92** 185501
- [8] Noël C M, Bossis G, Chaze A-M, Giulieri F and Lacis S 2006 *Phys. Rev. Lett.* **96** 217801
- [9] Ashkin A, Dziedzic J M, Bjorkholm J E and Chu S 1986 *Opt. Lett.* **11** 288
- [10] Svoboda K and Block S M 1994 *Ann. Rev. Biophys. Struct.* **23** 247
- [11] Loudet J C, Hanusse P and Poulin P 2004 *Science* **306** 1525
- [12] Chaikin P M and Lubensky T C 1995 *Principles of Condensed Matter Physics* (Cambridge: Cambridge University Press)
- [13] Mušević I, Škarabot M, Babič D, Osterman N, Poberaj I, Nazarenko V and Nych A 2004 *Phys. Rev. Lett.* **93** 187801